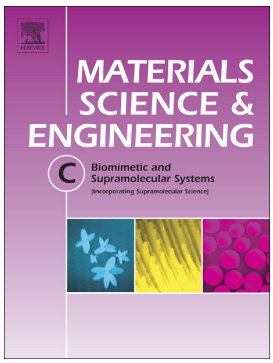

Injectable xyloglucan hydrogels incorporating spheroids of adipose stem cells for bone and cartilage regeneration

Emanuela Muscolino, Anna Barbara Di Stefano, Marco Trapani, Maria Antonietta Sabatino, Daniela Giacomazza, Francesco Moschella, Adriana Cordova, Francesca Toia, Clelia Dispenza

PII: S0928-4931(21)00685-8

DOI: https://doi.org/10.1016/j.msec.2021.112545

Reference: MSC 112545

To appear in: *Materials Science & Engineering C*

Received date: 19 August 2021

Revised date: 31 October 2021

Accepted date: 7 November 2021

Please cite this article as: E. Muscolino, A.B. Di Stefano, M. Trapani, et al., Injectable xyloglucan hydrogels incorporating spheroids of adipose stem cells for bone and cartilage regeneration, *Materials Science & Engineering C* (2021), https://doi.org/10.1016/j.msec.2021.112545

Injectable Xyloglucan Hydrogels Incorporating Spheroids of Adipose Stem Cells for Bone and Cartilage Regeneration

Emanuela Muscolino[a], *Anna Barbara Di Stefano*[b], *Marco Trapani*[b], *Maria Antonietta Sabatino*[a], *Daniela Giacomazza*[c], *Francesco Moschella*[b,d], *Adriana Cordova*[b,d], *Francesca Toia*[d], *Clelia Dispenza*[a,c,*]

[a]Dipartimento di Ingegneria, Università degli Studi di Palermo, Viale delle Scienze 6, 90128 Palermo, Italy.

[b]BIOPLAST-Laboratory of BIOlogy and Regenerative Medicine-PLASTic Surgery, Dipartimento di Discipline Chirurgiche, Oncologiche e Stomatologiche, Università degli Studi di Palermo, via del Vespro 129, 90127 Palermo, Italy.

[c]Istituto di Biofisica, Consiglio Nazionale delle Ricerche, Via U. La Malfa 153, 90146, Palermo, Italy.

[d]Dipartimento di Discipline Chirurgiche, Oncologiche e Stomatologiche, Università degli Studi di Palermo, via del Vespro 129, 90127 Palermo, Italy.

Corresponding author: Clelia Dispenza, tel. +39 091 23863710; email: *clelia.dispenza@unipa.it*

Abstract

Cartilage or bone regeneration approaches based on the direct injection of mesenchymal stem cells (MSCs) at the lesion site encounter several challenges, related to uncontrolled cell spreading and differentiation, reduced cell viability and poor engrafting. This work presents a simple and versatile strategy based on the synergic combination of in-situ forming hydrogels and spheroids of adipose stem cells (SASCs) with great potential for minimally invasive regenerative interventions aimed to threat bone and cartilage defects. Aqueous dispersions of partially degalactosylated xyloglucan (dXG) are mixed with SASCs derived from liposuction and either a chondroinductive or an osteoinductive medium. The dispersions rapidly set into hydrogels when temperature is brought to 37 °C. The physico-chemical and mechanical properties of the hydrogels are controlled by polymer concentration. The hydrogels, during 21 day

incubation at 37 °C, undergo significant structural rearrangements that support cell proliferation and spreading. In formulations containing 1%w dXG cell viability increases up to 300% for SASCs-derived osteoblasts and up to 1000% for SASCs-derived chondrocytes if compared with control 2D cultures. The successful differentiation into the target cells is supported by the expression of lineage-specific genes. Cell-cell and cell-matrix interactions are also investigated. All formulations resulted injectable, and the incorporated cells are fully viable after injection.

Keywords: spheroids of adipose stem cells; xyloglucan; injectable hydrogels; osteogenic differentiation; chondroblastic differentiation.

1. Introduction

Stem cells represent a great promise for tissue regeneration owing to their ability to self-renew and differentiate into specific tissue types. [1] In particular, mesenchymal stem cells are hugely attractive for tissue engineering and regenerative medicine interventions because of their relative ease of isolation from several tissues and overall multipotentiality. [2] In the presence of specific signalling cues, MSCs can differentiate in several mesenchymal lineages such as osteoblastic, chondroblastic, adipogenic, myogenic and endothelial cells. [2,3] The two major MSCs types are bone marrow stromal cells (BMSCs) and adipose stem cells (ASCs). Considering that subcutaneous adipose tissue has on average 1% of stem cells compared to the ca. 0.001% that are located in bone marrow, the adipose tissue is, in facts, the most convenient and accessible source of MSCs. [4,5]

ASC-based approaches for cartilage or bone regeneration are not without challenges. The direct administration of ASCs at the lesion site does not guarantee their engrafting and survival. Very often, only a small percentage (1-3%) of the administered stem cells are actually detected in the injection site one week after injection, with great discrepancies among different studies.[6,7] The survival rate is particularly low when MSCs are administered in harsh *in-vivo* environments, such as in the case of patients affected by chronic inflammatory or infective conditions.[8] In addition to that, when outside of their niche, adult stem cells quickly lose their developmental potential and

have the tendency to differentiate randomly. Therefore, artificial niches that can avoid uncontrolled cell spreading, preserve both stem cell viability and regenerative potential, and direct differentiation towards the desired cell lineage are sought. [9-11]

Hydrogels are very promising materials to engineer "MSCs-friendly" niches, because of their similarity to the natural tissue ECM in terms of water content and pore architecture, the possibility of providing cell-attachment sites and to be loaded with ECM proteins, sugars, and cellular secreted factors, such as growth factors, immunological factors and metabolic signals that can govern stem cell fate. By proper design of their chemical composition, morphology and mechanical properties, they can also actively contribute to either preserve the stemness or promote their differentiation towards a specific lineage, both *in vitro* and *in vivo*. [12-14] The intrinsic quality of the implanted stem cells is also a key factor for the success or failure of stem cell therapies.[15] Comparative studies on three-dimensional (3D) spheroids of adipose stem cells and canonical adipose stem cells in 2D adhesion cultures (ASCs), carried out both *in vitro* and *in vivo,* have highlighted significant differences between the two cell types for the different gene expression patterns and behaviours.[16,17] In adherent stem cells, disruption by trypsinization of cell-cell interactions, that are crucial for cell communication and cell-ECM commitment, have a profound effect on cells properties.[18] Conversely, spheroids of stem cell cultures show stemness properties and in appropriate conditions a more efficient mesenchymal differentiation. [19]

In a recent work, we demonstrated that stem cells isolated from lipoaspirate and cultivated as 3D spheroids, when incorporated in an *in-situ* forming, *ad-hoc* formulated soft hydrogel, were fully viable after 21 days of *in vitro* culturing and maintained intact their stemness.[20] The hydrogel matrix was obtained by mixing, at room temperature, equal volumes of the aqueous dispersion of a partially degalactosylated xyloglucan and a purposely compounded stem cell medium, increasing the temperature to human body temperature to induce the thermally-driven gelation. dXG derives from tamarind seed xyloglucan (XG) that is a non-ionic, water-soluble polysaccharide, composed of a β-(1,4)-D-glucan backbone, partially substituted by α-(1,6)-linked xylose unit, in turn partially β-D-galactosylated at O-2 (for the chemical structure see **Figure S1** of Supporting information).[21] Being a storage polymer for the embryo, XG is found in tamarind seeds at a relatively high concentration, can be extracted via simple and economic viable procedures, in good yields and high purity. XG is also active in tissue

regeneration, being recognized by β-galactose binding galactins, triggering keratinocyte adhesion and promoting skin re-epithelialization and wound healing.[22,23] Xyloglucan with degalactosylation degree of ~45% undergoes a reversible sol-gel transition at ~37°C. [24,25]

With this work, we report on an important step forward in the development of a SASCs/dXG hydrogel platform for minimally invasive regenerative medicine interventions. We aim to demonstrate that, varying dXG concentration and the composition of the cell culture medium, the morphological, mechanical and functional properties of dXG hydrogels can be engineered to create "SASC-friendly", pre-programmed niches that can drive differentiation towards the desired cell lineage; in this case osteogenic or chondrogenic. We explored the ability of the hydrogels to evolve in time and remodel their network to support of SASCs-derived cell proliferation and spreading. We started a more in-depth investigation on SASCs-derived cell expression of markers regulating cell-matrix and cell-cell interactions. Finally, we measured SASC-laden dXG dispersion viscosities, the pressure to be applied for their extrusion through a small gauge syringe and evaluated the impact that this process has on the hydrogel structure and cell viability.

2. Experimental

2.1 Materials

Tamarind seed xyloglucan was purchased from Megazyme International (Ireland), β-Galactosidase from Aspergillus oryzae (11.8 U/mg) was purchased from Sigma Chemicals (USA). Tamarind seeds xyloglucan was degalactosylated (dXG) according to an established protocol, to obtain a degalactosylated degree of ca. 45% [26] Sugar composition of the tamarind seed xyloglucan is xylose 34 %w; glucose 45 %w; galactose 17 %w; arabinose and other sugars 4 %w, as provided by the supplier.

2.2 Cell cultures

Adipose tissue samples were obtained from healthy subjects. Institutional ethical board approval and patient consent was obtained for the use of tissue samples prior to the research (AOUP "Paolo Giaccone", Palermo, Italy – Project code: GR-2016-02364931). Lipoaspirate samples were harvested from different anatomical parts such

as the trochanteral region, abdomen, breast, flanks and hips. Then, they were digested mechanically (30 minutes at 37 ° C under stirring) and enzymatically (collagenase 150 mg / ml, Gibco, Carlsbad, CA). After centrifugation at 1200 rpm for 5 minutes, the stromal vascular fraction (SVF) was recovered and resuspended in stem cell medium and in ultra-low attachment culture flasks (Corning, NY). After spheroids isolation, they were plated in adherent conditions for chondroblastic or osteoblastic differentiation according to StemPro® Chondrogenesis Differentiation kit or StemPro® Osteogenesis Differentiation Kit protocols (Invitrogen) and maintained at 37°C in a humidified 5% CO_2 incubator for 7, 14 and 21 days.

2.3 dXG Dispersion Preparation

dXG powder was added to 0.22 µm pre-filtered water, at 2 %w, 3 %w and 5 %w concentration, and stirred for about 2 hours at 5°C until a homogenous dispersion was obtained. Afterwards, the dispersions were sterilized by autoclaving at 121°C for 20 minutes. Dispersions were stored at 4°C.

2.4 Hydrogel Preparation

Known volumes of the 2 %w, 3 %w and 5 %w dXG polymeric dispersions were gently mixed with the same volume of water, or chondrogenesis differentiation medium or with the osteogenesis differentiation medium and then incubated at 37 °C for 10 min before any further use. The incubation conditions are the same described in section 2.3.

2.5 Rheological analysis in small-oscillatory conditions

2.5.1 Gel time measurements

Gel times were measured using a stress-controlled Rheometer AR G2 (TA Instruments). A plate-plate geometry was used with the upper acrylic plate of 40 mm diameter. The gap was set at 500 µm, the strain at $1x10^{-3}$, and the frequency at 1 Hz. Known volumes of the formulations were placed on the bottom plate and surrounded by silicon oil to prevent evaporation.

2.5.2 Dynamic mechanical spectra

The dynamic mechanical spectra were determined using a stress-controlled Rheometer AR G2 (TA Instruments). The geometry used was a PIK anti-slippery plate of 20 mm diameter and the gap was set in the range 500-1000 µm.

Strain sweep measurements were performed to explore the extension of the linear viscoelastic range, at 1 Hz, and identify the optimum strain conditions for the subsequent frequency sweep tests. Frequency sweep measurements were also performed at constant strain in the range between $7x10^{-3}$ and $1x10^{-2}$, depending on the system, and the frequency was swept between 0.1 Hz and 10 Hz. Known volumes of the formulations were either placed or injected on the bottom plate and the measurements started after 10 minutes of thermal and structural equilibration at the measurement temperature of 37.0±0.1°C, controlled by a built-in Peltier system. Measurements were carried out in triplicate from independent preparations. The represented plots of G' and G" are the arithmetic average of the three curves.

2.6 Morphological Analysis

Hydrogel microstructure was investigated using a Field Emission Scanning Electron Microscope Phenom ProX desktop at an accelerating voltage of 10kV. The hydrogels were frozen in liquid nitrogen, freeze-dried, mounted on aluminium stubs and gold coated by JFC-1300 gold coater (JEOL) for 120 s at 30 mA before scanning.

2.7 Swelling/Erosion Evaluations

Hydrogels (ca. 0.5 ml) were produced for each formulation in suitable moulds. Samples were weighed with a precision balance, then placed on glass cylinders with a porous bottom, immersed in a bath filled with a large excess isotonic PBS and 0.02%w NaN_3 as preservative and maintained at constant temperature of 37°C. Samples were taken out from the solution at predetermined time intervals, carefully blotted and weighted. The Weight Change (WC %) was determined as:

$$WC = \frac{W_t - W_i}{W_i} \times 100$$

where W_t is the weight of the hydrogel at time t and W_i is the initial weight. Reported data are the average of 6 samples.

2.8 Stem Cells Loading, Incubation and Recovery

Cells were loaded by mixing the 2 %w, 3 %w and 5 %w dXG polymeric dispersions with the same volume of SASC suspension in either CDM or ODM (named after as dXG1-

C/O-SASCs, dXG1.5-C/O-SASCs and dXG2.5-C/O-SASCs), respectively. 50,000 cells/well were loaded and maintained in a CO_2 incubator at 37 °C for 7 days, 14 days and 21 days.

The recovery of cells was performed by incubation in 84 U/ml aqueous solution of Cellulase from *Trichoderma reesei* (Sigma Aldrich) for 90 min at 37 °C, centrifugation at 1200 rpm for 5 min at 4 °C and removal of the supernatant dispersion. In order to evaluate eventual effects of the enzymatic treatment on cells, the same protocol was applied to SASCs and their viability was confirmed by cell count with trypan blue.

2.9 Colonization Analysis

To observe scaffold colonization, SASC-laden hydrogels were inspected under the light and fluorescence microscope (Leica DM IL LED Fluo) after 21 days culture. In particular, for the fluorescence analysis, 500000 cells/ml per well were labelled with the cell membrane PKH26 dye (MINI26, Sigma Aldrich).

2.10 Cell Viability Analysis

Cell viability of SASCs in all conditions was quantified with MTS test (3-(4,5-dimethylthiazol-2-yl)-5-(3-carboxymethoxyphenyl)-2-(4-sulfophenyl)-2H tetrazolium) (Promega). Cells were plated in biological triplicates at a density of 50000 cells/well in 96-well plates filled either with 100 µl/well of culture medium (control) or 50 µl/well of hydrogel and 50 µl/well of culture medium. The absorbance at 490 nm was analysed at 7 days, 14 days and 21 days of incubation through TECAN Spark 10M spectrophotometer.

2.11 mRNA Expression Profile

Total RNA was extracted from SASCs recovered from the hydrogel using RNeasy Mini Kit (Qiagen) and quantified using Qubit4 (Invitrogen) fluorometer. The RNA (175 ng) was retrotranscribed in cDNA through the High Capacity cDNA Reverse Transcription kit (Applied Biosystems). The qPCR reactions were all performed in triplicate. The predesigned Taqman primers (Thermo Fisher) were RUNX2 Hs00231692_m1 and ALP Hs01029144_m1 as osteoblastic markers; SOX9 Hs01001343_g1 and Col10A1 Hs00166657_m1 as chondroblastic markers; and GAPDH Hs02758991_g1 as housekeeping gene. In addition, CDH1 Hs01023895-m1 and

ITGB1BP1 Hs01555790_g1 were analysed for cell-cell and cell-matrix interactions. The relative expression levels of mRNAs were calculated using the 2−ΔΔCt Livak method.[27]

2.12 Immunofluorescence Staining

In order to characterize the SASCs differentiation after 21 days of culture in CDM or ODM, cells were recovered from the hydrogels as described in section 2.9 and plated on slides for immunostaining analysis. The cells were fixed in 4% formaldehyde for 10 min at room temperature (RT). Then, they were permeabilized with Triton-X100 0.1% and exposed to either rabbit anti-human RUNX2 or SOX9 antibodies (SantaCruz) overnight at 4 °C. After incubation to Goat Anti-Rabbit, Alexa fluor Plus 568 and Goat Anti-mouse, Alexa Fluor Plus 488 (Thermofisher Scientific) secondary antibodies for 2 h at RT, the nuclei were counterstained with Hoechst for 10 min at RT. The immunofluorescence analysis was conducted with confocal microscope.

2.13 Statistical Analysis

Data are expressed as mean± standard deviation of three independent experiments. Statistical significance was calculated using one-way analysis of variance (ANOVA), followed by either a Tukey's or Bonferroni's multiple comparison post hoc test. Significance levels were analysed with GraphPad Prism5 statistical software and indicated as p values (*$p < 0.05$, **$p < 0.01$, and ***$p < 0.001$).

2.14 Injectability

As part of the injectability assessment different type of measurements were carried out: (i) shear viscosity as function of shear rate measurements (flow curves); (ii) rheological analysis in small-oscillatory conditions; and (iii) force-displacement plots of formulations pre-loaded in syringes.

The flow curves of the dispersions formulated with ODM and CDM, with and without SASCs (500000 cells/ml), were obtained using the stress-controlled Rheometer AR G2, operating in rotational mode at the constant temperature of 25.0±0.1°C. Measurements were performed with the PIK anti-slippery of 20 mm diameter and a gap of 1000 μm.

Force-displacement plots were obtained with an Instron Universal Uniaxial Testing Machine 3365 equipped with 1/1000 N load cell capacity, in compression mode, by

applying a constant displacement rate (40 mm/min equivalent to 5,30 mL/min) to the plunger of the syringe and measuring the resulting force (F) as function of the displacement. The syringe was immobilized with a metal clamp. The injection was carried out with 2.5 ml polypropylene syringes equipped with an G23 needles, loaded with cell-laden and cell-devoid dispersions. All experiments were performed after the systems were stored at 4°C for 24 h and thermally equilibrated at room temperature for 1 h. The influence of the specific set up and the friction of the plunger was preliminarily evaluated by filling the syringe with water and extruding it in air. The plug force of the dispersions was measured by extrusion of the material in air. The results are expressed in terms of force, F, vs 1 – ε, that is the normalized travelled distance, where ε is representing the ratio (Td-D)/Td, where Td is the maximum distance the plunger can physically travel, and D is the distance travelled.

The rheological analysis in small-oscillatory conditions was carried out on samples, with and without SASCs (500000 cells/ml), directly injected on the rheometer plate at ca. 20°C and let equilibrate at 37°C for 10 minutes. Details on the experimental parameters are provided in section 2.4. A cell viability analysis was performed by MTS test after extrusion of the cells (500000 cells/ml) mixed with dXG dispersions through 1.0 ml polypropylene syringes equipped with an G23 needles. The systems were placed in 96 multiwell and cultured for 24 hours. The absorbance was determined in a spectrophotometer at 490 nm.

3. Results and Discussion

3.1. Experimental design

In **Figure 1**, the approach followed for the preparation and evaluation of SASC-laden injectable dXG formulations is shown. Briefly, (i) adipose tissue was harvested from lipoaspirate of volunteer donors; (ii) SASCs were isolated from the adipose tissue and cultured in ultra-low adhesion flasks with a stem cell medium; (iii) dXG aqueous dispersions were prepared at three concentrations (2 %w, 3 %w and 5 %w) and mixed only with equal volumes of either a chondrogenesis differentiation medium (CDM) or an osteogenesis differentiation medium (ODM), or with one of the two media and SASCs; (iv) both SASC-free and SASC-laden dXG hydrogels were incubated at 37 °C up to 21 days; (v) SASC-free systems were characterized for their mechanical properties by small

amplitude oscillatory rheological measurements and for their morphology via scanning electron microscopy (SEM) as prepared (T0), after 7 days (T7), 14 days (T14) and 21 days (T21) of incubation; the swelling and erosion behaviour of T0 systems was investigated by measuring weight changes upon immersion in a large volume of isotonic phosphate buffer; (vi) SASC-laden hydrogels were evaluated for scaffold colonization ability, cell viability, effect of differentiation on mRNA expression, cell-cell and cell-matrix interactions genes. Both SASC-free and SASC-laden hydrogels were characterised for injectability.

Three different polymer concentrations with meaningful differences in their mechanical properties from the rheological evaluation were analysed. The hydrogel systems are named after as dXGy-z, where y indicates the final polymer concentration in weight percentage (1 %w, 1.5 %w and 2.5 %w) and z is a letter referring to the medium that has been mixed with the dXG aqueous dispersion. In particular, W stands for water (used as reference medium), C for CDM and O for ODM. To identify SASC-laden hydrogels the acronym SASCs follows the hydrogel name (dXGy-z-SASCs).

The incubation time will be referred as T0 for the systems that are analysed 10 min after preparation, T7, T14 and T21 for the systems that are analysed after 7 days, 14 days and 21 days of incubation at 37 °C, respectively.

In general, dXG dispersions that lead, after mixing with the inductive medium, to a final polymer concentration below 1 %w yield gel flakes rather than uniformly gelled systems. Hence, they are less reproducible and more difficult to control in terms of their ability to host cells. For this reason, polymer concentrations below 1 %w were not taken into consideration for this study.

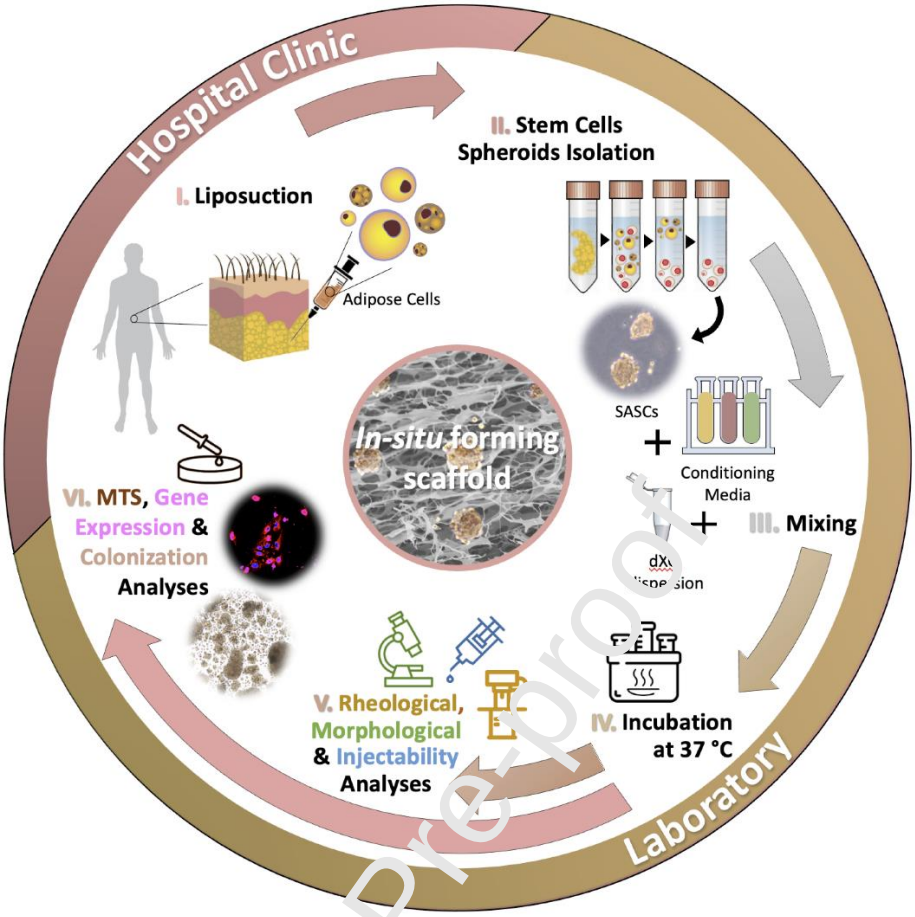

Figure 1. Graphical representation of the experimental strategy. (I) Harvesting of adipose tissue by liposuction; (II) SASC isolation and culturing in 3D conditions; (III) aqueous dXG dispersions mixing with either a chondroinductive (CDM) or osteoinductive medium (ODM), or with one of the two media and SASCs; (IV) incubation of both SASC-free and SASC-laden dXG hydrogels at 37 °C up to 21 days; (V) physico-chemical, rheological and morphological characterisation of SASC-free systems; (VI) in-vitro evaluations of SASC-laden hydrogels.

3.2 The influence of conditioning media on hydrogels structure formation and evolution

The influence of the conditioning media on dXG network organization was investigated by rheological measurements in small amplitude oscillation conditions.

Two type of measurements were performed. Storage modulus, G', and loss modulus, G'', measurements as a function of the time at a fixed strain and frequency (time sweeps), performed immediately after mixing to determine the time to gel. Frequency sweep tests at fixed strain to characterise the networks after conditioning the hydrogels

in unperturbed conditions with water or with the chondroinductive or the osteoinductive medium for various time periods (T0, T7, T14 and T21). Both time sweeps and frequency sweeps were carried out at constant temperature of 37±1°C.

In **Figure 2A-C** time sweeps are shown. dXG1 systems show an initial tract when G' increase and G" is rather constant, therefore at a given time there is a crossover with G' becoming equal to G". Subsequently, G' continues to increase at a slower rate. The crossover time can be assumed as the gel time (t_g). None of these systems reach a plateau value of the storage modulus (end of the cure). The network is indeed formed, as indicated by the stepwise increase of the elastic component of the complex modulus, but the hydrogels do not attain a reference network structure during the 60 min of the analysis. It can be anticipated that none of these systems reach as an equilibrium structure even after much longer incubation times at 37°C.

The medium composition has an influence t_g. Both dXG1-C and dXG1-O have longer gel times than dXG1-W. In particular, t_g is 13 min for dXG1-W, 14 min for dXG1-C and 18 min for dXG1-O. G' and G" curves for dXG1-O start from one order of magnitude lower values than for dXG1-W. This evidence suggests that the solutes present in the inductive media (salts, glucose and amino acids), and more particularly those present in OCM, perturb dXG chain association in condensed domains and the physical gelation process. Being dXG sol-gel transition mainly driven by hydrophobic and hydrogen bonding interactions, the presence of ionic, polar and hydrophobic solutes can affect polymer-polymer and polymer-solvent interaction landscape, introducing depletion interactions and polymer-solute hydrophobic effects. An influence of the medium was also observed when aqueous dXG was mixed with the medium that was specifically formulated to preserve cell stemness.[7,10]

Also for dXG1-C and dXG1-O, G' curves do not reach a plateau. Increasing the polymer concentration reduces the gel time. dXG1.5-W is characterised by G' > G" from the beginning of the measurement, while t_g for both dXG1.5-C and dXG1.5-O is 3 min. All dXG2.5 systems are characterised by G'>G" in the entire time span observed, meaning that the onset of gelation at this temperature occurs during the acquisition of the first data point. Also for the more concentrated systems, plateau values of G' are not rigorously attained (**Figure 2D-F**).

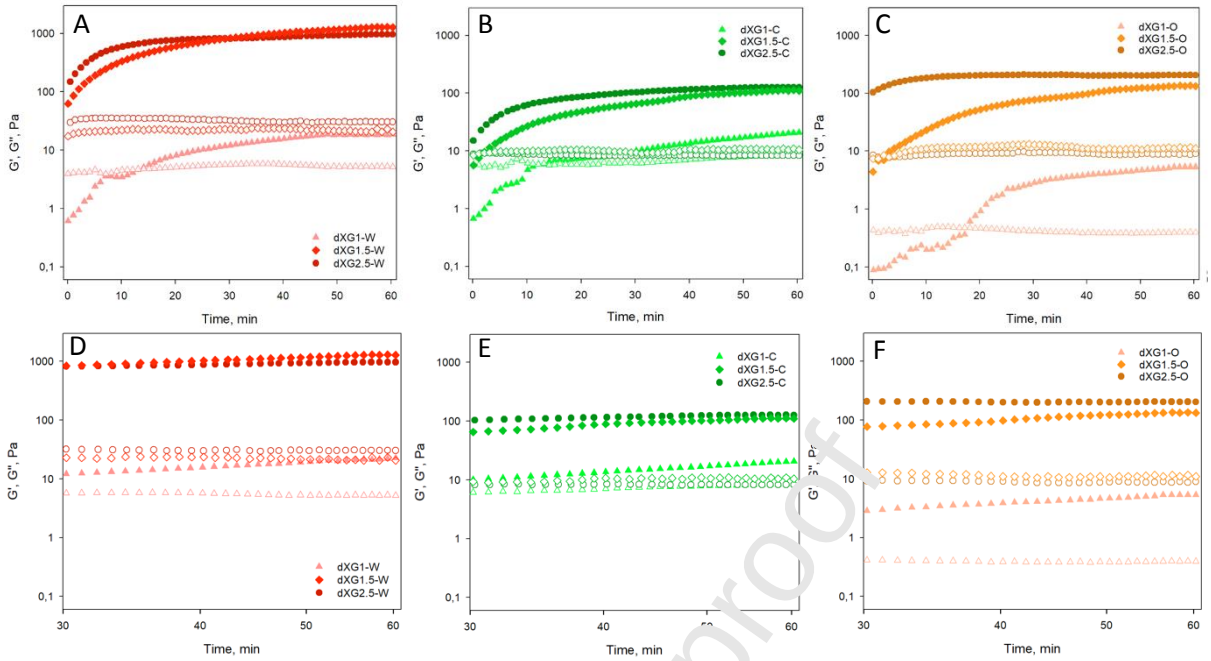

Figure 2. Storage modulus, G' (full dot), and loss modulus, G" (hollow dot), as a function of time for dXG hydrogels conditioned with water (A), CDM (B) and ODM (C); Semi log plot of the storage, G' (full dot), and loss, G" (hollow dot) moduli as a function of time in the interval 30 - 60 min for dXG hydrogels conditioned with water (D), CDM (E) and ODM (F)

G' G" curves as a function of the frequency are reported in **Figure 3A-I** for the hydrogels as produced (T0) and after 21 days (T21) of incubation. The frequency average G' values (G'_{av}) in the 0.5 Hz - 5 Hz interval for T0, T7, T14 and T21 systems are reported in **Figure 3J-L.** In particular, **Figure 3A-C** shows the rheological behaviour of the three systems with the lowest polymer concentration, dXG1-W, dXG1-C and dXG1-O. For all three systems, at T0, G' curve is higher than G" curve and they are both frequency dependent. These rheological features are characteristic of weak gels with structural heterogeneities. dXG1-W has slightly higher storage modulus (G'av ~90Pa) than dXG1-C (G'av ~70 Pa) and dXG1-O (G'av~60 Pa) (**Figure 3J**). At T21, G' and G" values become essentially almost frequency independent for all systems. This indicates that the systems have developed a more uniform network. Looking at the evolution of the systems with time (**Figure 3J**), statistically relevant changes of G' values can be noted

especially for dGX1-O, that is the system characterised by lowest initial G' and G" values also from the time sweep tests. The weaker is the initial network configuration the easier is for the system to undergo a maturation phase where, by activation of chain segment dynamics, the extent and density of physical crosslinking is modified. This maturation can show effects on the stiffness (related to G') and the damping characteristics (related to G") of the hydrogel and, as already observed, on the homogeneity of the network structure (frequency dependence of G' and G"). It is followed by a subsequent remodelling phase, that results from highly cooperative motions of chains with slower dynamics, leading to further significant changes of G' and G" values from T7 to T14, and less pronounced from T14 to T21.

Figure 3D-F shows the rheological behaviour of dXG1.5 systems. For all these systems, G' curve is higher than G" curve and both curves are already less frequency dependent at T0 than those of the dXG1 systems. At T21 the curves also become frequency independent.

The dXG2.5 systems (**Figure 3G-I**) show a marked increase of G' and G" curves from T0 to T21 alongside with flattening of the curves. **Figure 3L** shows that the increase of G' is monotonic for dXG2.5-C and dXG2.5-O. Despite of their higher polymer concentration, these systems initially form hydrogels that are weaker than the dXG1.5 ones, probably due to their higher viscosity in the sol state (as it will be shown in section 2.5), which hinders chain mobility and delays the formation of a well-interconnected network. Prolonged incubation in this case not only reduces the heterogeneities in the network but make the network stronger.

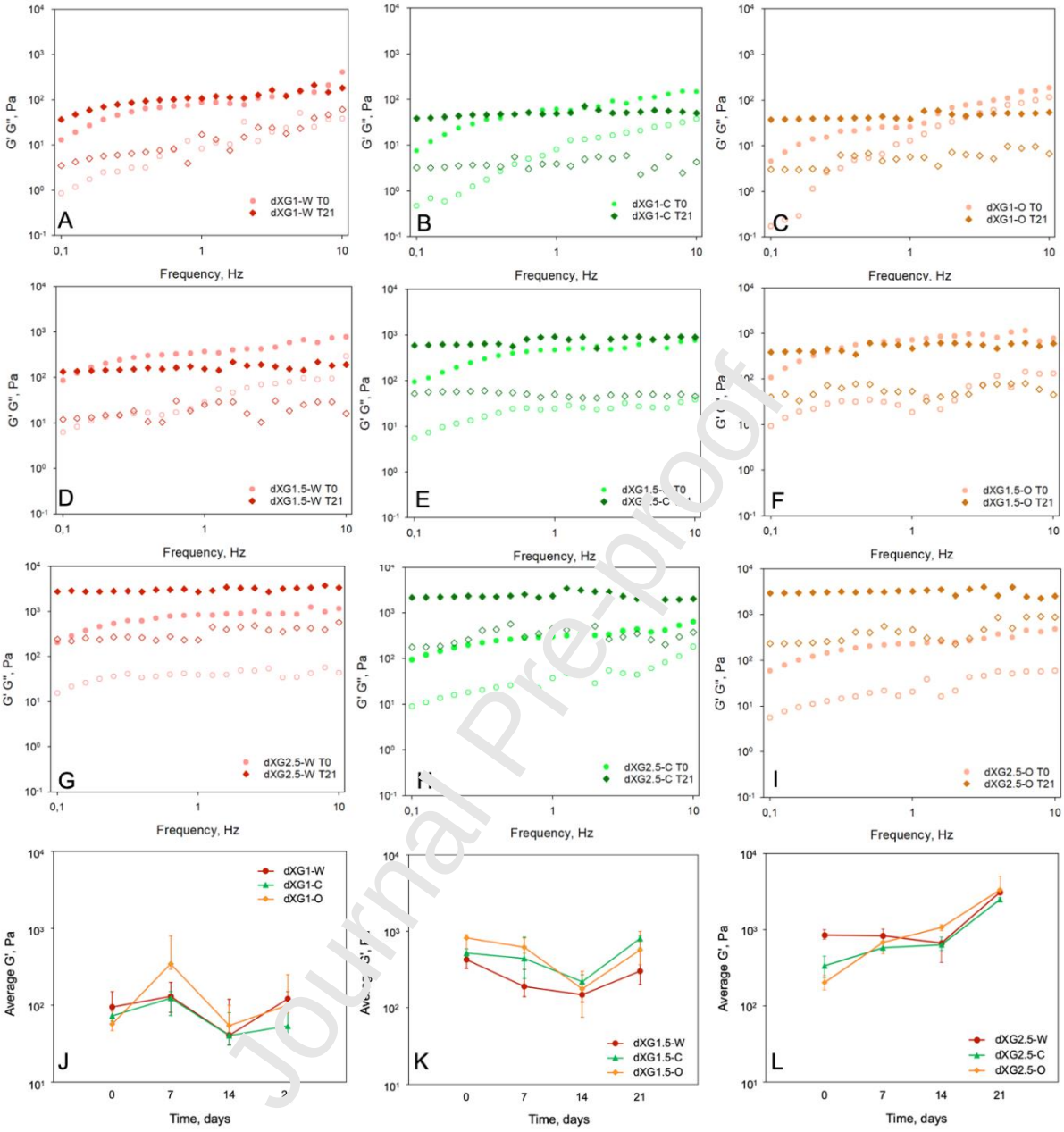

Figure 3. Storage modulus, G' (full dot), and loss modulus, G" (hollow dot), of dXG1 (A-C), dXG1.5 (D-F) and dXG2.5 (G-I) hydrogels conditioned with water, CDM and ODM, at T0 and T21 as function of frequency. Average G', of dXG1 (J), dXG1.5 (K) and dXG2.5 (L) hydrogels conditioned with water, CDM and ODM, at T0, T7, T14 and T21.

The morphology evolution of the various systems was investigated by SEM analysis of the freeze-dried solids produced after quenching the samples in liquid nitrogen. None of systems formulated with only water underwent significant volume changes upon freeze drying. Contrarywise, all systems mixed with inductive media underwent volume contraction after lyophilisation, the more significant the lower was the polymer concentration.

Figure 4 shows the SEM micrographs of the dXG1 hydrogel cross-sections at T0, T7, T14 and T21. The dXG1-W T0 hydrogel shows a uniform porous structure formed by shreds of very thin membranes connected by filaments. The average pore size is around 10 μm. From T0 to T7, the system shows an increased tendency of forming planar membranes, that become stacked lamellae at T14. At T21 dXG1 has evolved towards a heterogenous open porous structure, with thicker wall pores and average pore size of about 70 μm.

The morphological analysis of the systems formulated with ODM and CDM supports the strong effect of the conditioning media on the network organization and their evolution with time that was appraised also with the rheological analysis. A T0, both the dXG1-O and dXG1-C systems show a heterogenous fibrous structure, formed by thick and intertwined threads. At higher magnification (see **inset of dXG1-O**), corrugated surfaces and protruding salt crystals are also evident. At T7, more uniformly porous solids are obtained, probably due to the formation of more extended networks. In particular, the porosity is open and interconnected for dXG1-C, tighter for dXG1-O. The pronounced change in morphology for dXG1-O can explain the observed significant increase of storage modulus for this system at T7. At T14 and T21, both dXG1-O and dXG1-C have evolved into a more open porous structure, that is in good agreement with the reduction of their G' values, and hence their stiffness, with respect to T7.

Figure 5 and 6 displays the SEM morphologies of dXG1.5 and dXG2.5 hydrogels, respectively. The morphologies of dXG1.5-W and dXG2.5 W at T0 are not too different from the one of the dXG1-W T0 in terms of average pore size. dXG1.5-W T0 shows thin filaments and some wider shredded membranes, while dXG2.5-W T0 presents a porous structure with slightly thicker pore walls. The presence of extended condensed domains of polymer chains at the increase of polymer concentration is in good agreement with the observed increase of storage modulus. During the incubation, the tendence of dXG to self-assemble in ribbon-like aggregates and membranes is more and more evident. [28,20]

This phenomenon is more pronounced for dXG2.5-W T21, that shows a fairly compact structure with partially occluded porosity.

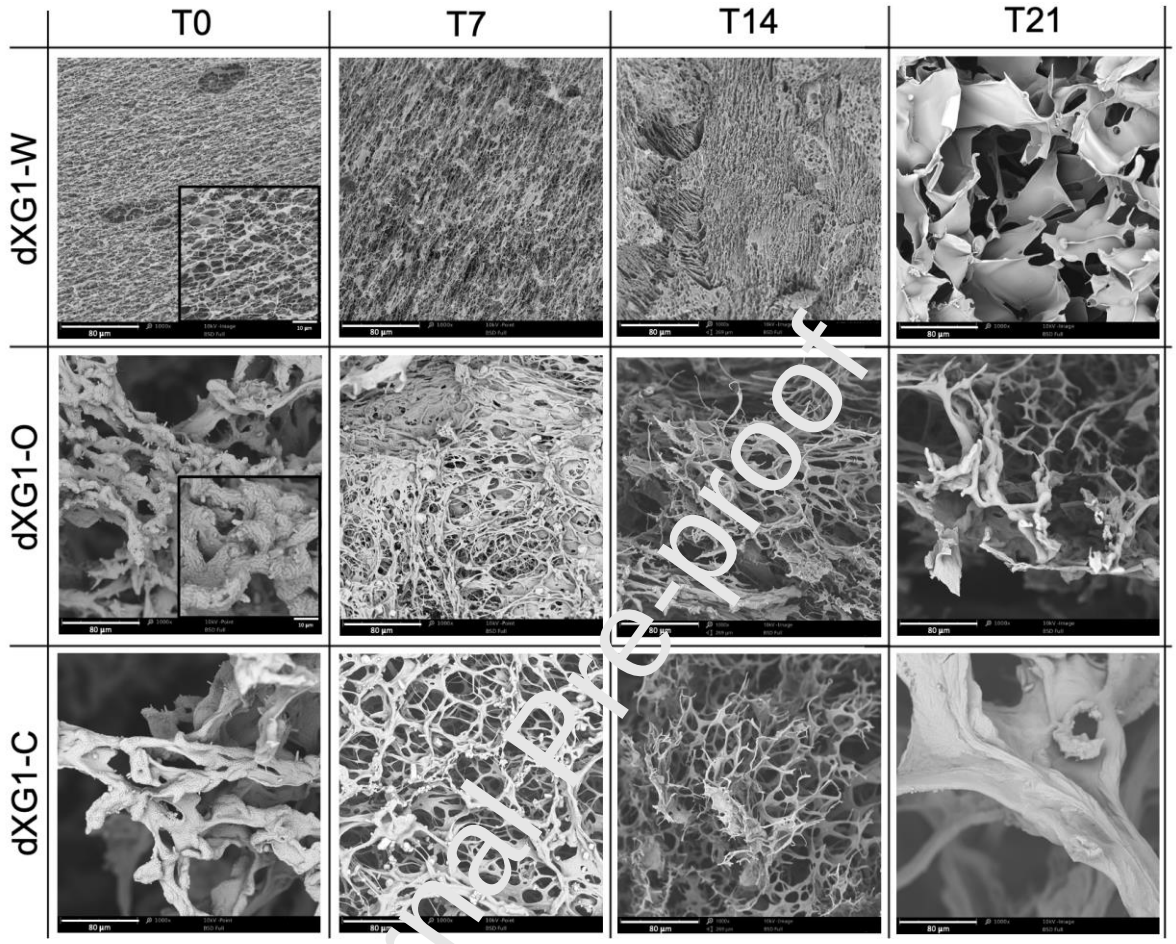

Figure 4. SEM micrographs (cross-sections) of dXG1 hydrogels conditioned with water, ODM and CDM, at T0, T7, T14 and T21 (scale bar 80 μm). For dXG1-W and dXG1-O, insets with SEM micrographs at higher magnification were included (scale bar 10 μm).

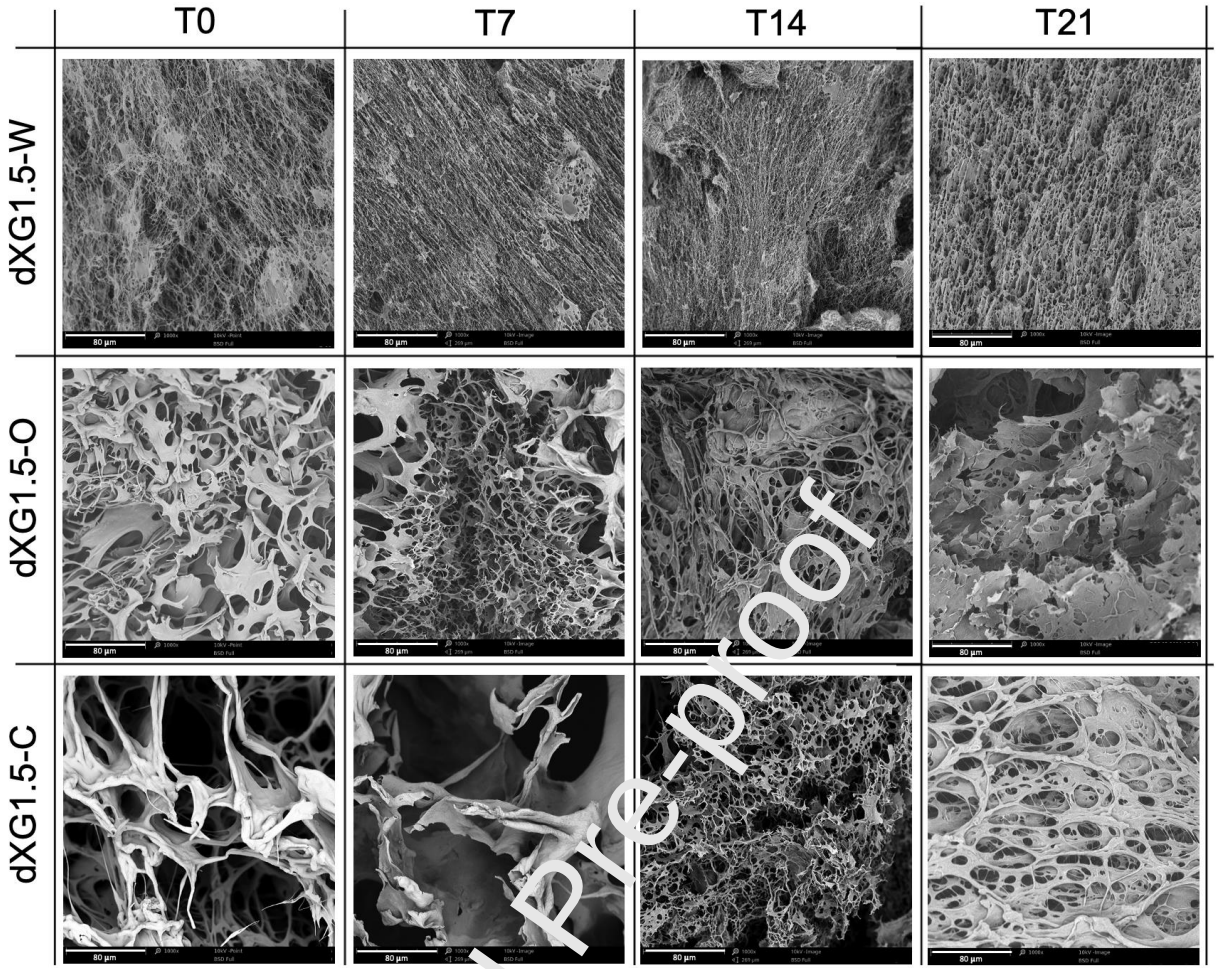

Figure 5. SEM micrographs (cross-sections) of dXG1.5 hydrogels conditioned with water, ODM and CDM, at T0, T7, T14 and T21 (scale bar 80 μm).

Differences in morphology varying the conditioning medium at T0 are also shown for these systems characterized by higher polymer concentration, but they are less pronounced for dXG2.5 than for dXG1.5. This is expected considering that the polymer content in the system increases while the concentration of the other solutes, coming from the conditioning media, is constant. The pores clearly appear as holes in membranes. The pore size distribution and the thickness of the membranes are affected by the nature of solutes other than dXG. CDM introduces the strongest perturbation in dXG self-assembly yielding structures with larger pores. Unfortunately, the exact composition of the conditioning media is proprietary and not known to the authors of this work. This prevents the possibility of ascribing the observed phenomena to specific ions or molecules present in the systems. The dXG1.5 and dXG2.5 systems formulated with the inductive media develop with increasing the incubation time a less heterogeneous and more structured morphology, similarly to the systems conditioned

with water and in agreement with the increase of the viscoelastic parameters. At T21 the differences between the two media are less important although still present, so are the differences in G' and G" curves, especially for dXG2.5.

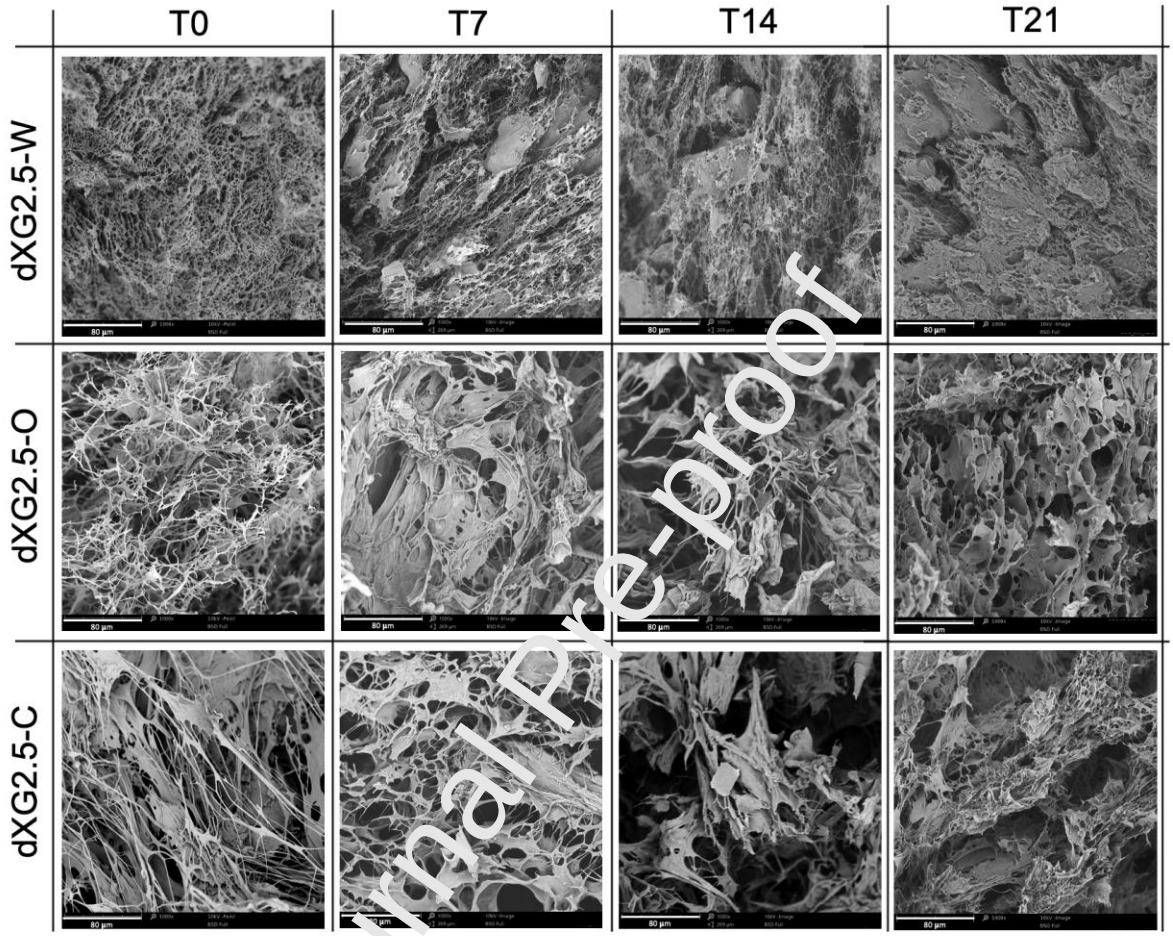

Figure 6. SEM micrographs (cross-sections) of dXG2.5 hydrogels conditioned with water, ODM and CDM at T0, T7, T14 and T21 (scale bar 80 μm).

The hydrolytic stability of the hydrogels pre-conditioned at 37°C with the various media for 3 h was evaluated by immersing cylindrical samples of each system in a large excess of isotonic phosphate buffer at 37°C. In **Figure 7A-C** the average mass change as function of the immersion time is reported. It is worth pointing out that the porous sept of the sample holders is able to retain only the macroscopic portions of the hydrogels (cut-off approx. 1 mm), while micro/nano gel fragments can pass through the sept. As shown in **Figure 7A**, dXG1-O and dXG1-C systems were fully eroded at 21 days. For hydrogels produced at 1.5 %w and 2.5 %w with water or with ODM (**Figure 7B-C**), the erosion behaviour is similar and the residual mass after 28 days is around 60-65 %w,

for the systems conditioned with water, and around 35-40 %w, for the systems conditioned with ODM. The dXG1.5-C resembles more the corresponding dXG1-C, while the dXG2.5-C is more similar to dXG2.5-O. In conclusion, at low polymer concentration the erosion resistance is lower and less affected by the nature of medium used for the pre-conditioning treatment. This is probably due to the lower crosslinking density and/or the more transient nature of the crosslinking points, as suggested by the frequency-dependent G' and G" curves. At higher polymer concentration, condition that would favor chain self-assembly in extended associated domains and formation of tougher networks, the perturbation introduced by the solutes of the conditioning media becomes more significant and reduce the interconnections among polymer chains. We can speculate that the hydrophilic solutes (including hydrated ions) compete for hydration water and promote the confinement of the polymer chains in segregated domains; at the same time, hydrophobic low molecular factors (growth factors) associate with the polymer chains competing with polymer-polymer associations.

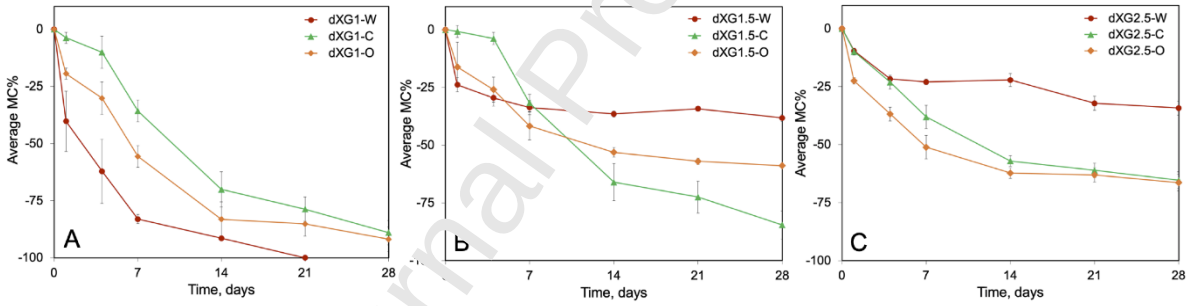

Figure 7. Average mass change percentage (MC%) of dXG1(A), dXG1.5 (B) and dXG2.5 (C) hydrogels conditioned with water, ODM and CDM.

3.3 Biological evaluation of osteoblastic differentiation

In order to investigate if the hydrogel can support the osteoblastic differentiation of SASCs, fluctuating spheroids suspensions (50000 cells) were labelled with PKH26 red dye, a cell membrane vital label, slowly mixed in ODM with equal volumes of each of the three dXG dispersions and finally incorporated in hydrogels by incubation at 37°C. The influence of the presence of dXG scaffolds on SASCs differentiation was evaluated by morphological, proliferation and specific differentiation analyses.

Cell morphology in the systems was inspected under both light and fluorescence microscopes. **Figure 8A** shows the typical morphology of SASCs at T0, comprising smaller and larger spheroidal aggregates as well as single cells. After 21 days of *in vitro* osteoblastic culture (see **Figure 8B**), the cells are uniformly distributed on the surface but also through the thickness of the hydrogel, as visible by the immunofluorescence analysis of the pre-labelled cells.

The viability of the SASCs was quantified by MTS analysis carried out on cell-laden hydrogels at three time points of *in vitro* culture: T7, T14 and T21 (see **Figure 8C**). At T21, when we expect that the differentiation has taken place, we observe an increase of cell viability over the value obtained for the SASCs cultured with ODM without the hydrogel. In particular, we see a ~3-fold increase for dXG1-O-SASCs and a ~1.5-fold increase for both dXG1.5-O-SASCs and dXG2.5-O-SASCs. We notice that at T7 instead, SASCs incorporated in dXG1-O and dXG1.5-O experienced a 75% reduction of cell viability. This effect is prolonged to 14 days for dXG1.5-O-SASCs. A reduction of viability, yet much less severe (of ~ 30%), was also shown for dXG2.5-O-SASCs. Interestingly, the systems that experienced the most dramatic decrease in cell viability were also characterised by a subsequent fast proliferation phase. The dXG2.5-O-SASCs system that mostly retained cell viability is characterised by a lower growth rate. Different possible concurrent causes could be at the basis of this behaviour. We can imagine that during the initial phase of the differentiation process, a natural selection of cells in the spheroids occurs that results in the viability of the only fraction that is capable of differentiating towards osteoblasts. We can also argue that dXG-O hydrogel networks at T7 are still too tight to guarantee the optimal conditions for cell spreading and scaffold colonization (e.g. see dXG1-O T7 in **Figure 4**). In particular for dXG1-O, we observed that prolonging the incubation at 37°C together with the culture medium induces a remodelling of the network architecture and opens larger and interconnected pores that may represent more favourable conditions for cell growth and spreading.

In order to confirm that the osteoblastic differentiation has occurred, molecular investigations of RUNX2 (Runt-related transcription factor 2 gene) and ALP (alkaline phosphatase) were performed on both control cells and cells recovered from the hydrogels at T21 of *in vitro* culture. RUNX2 is the primary transcription factor in bone formation. It plays a vital role during osteoblast differentiation and regulates the downstream expression of several osteoblast markers and bone matrix genes.[29] ALP is

an enzyme involved in the late osteoblastic differentiation, bone formation and mineralization.[30] These genes were chosen in accordance with the miRNA and mRNA expression study carried out on the same type of SASCs,[19, 31] that identify them as representative markers of osteoblastic differentiation. The real-time PCR analysis revealed a massive increase of RUNX2 expression, that is ~120-fold for dXG1-O ($P < 0.001$), ~50-fold for dXG1.5-O and ~10-fold for dXG2.5-O, over the value obtained for SASC-derived osteoblasts in scaffold-free conditions (CTR). RUNX2 was correlated with the proliferation of mesenchymal stem cells and osteoblast progenitors as well as with their differentiation;[29] this could explain a possible correlation between the increased cell viability and the upregulation of RUNX2 expression in dXG-O, and particularly in dXG1-O. The mRNA ALP levels analysis showed a similar trend to the RUNX2 one, with a ~7-fold increase for dXG1-O and ~2-fold increase for the other two systems (**Figure 8D**). ALP is related to active bone formation with a peak of expression during osteoblastic maturation, as at T21 in our study, and then a decline during osteocytic transformation.[32] Then, we analysed the protein expression of RUNX2, the overexpressed marker in our systems, through immunofluorescence analysis. The z-stack visualization of confocal microscopy images confirmed the presence of RUNX2 positive cells in all systems (**Figure 8E**). The ability of SASCs to differentiate toward osteoblastic lineage has already been demonstrated,[19] while here we provide evidence that SASCs display a greater osteoblastic differentiation potential when they are placed together with the dXG hydrogels obtained at all three polymer concentrations.

The maintenance of stemness conditions and the higher viability of undifferentiated SASCs in comparison to their 2D-counterpart, that was shown in our previous study, confirmed the substantial difference in behaviour between two populations of cells, that is related to different expression patterns of mRNAs and proteins.[20] Now, we intend to demonstrate that SASCs embedded in dXG-based artificial niches have also better differentiation abilities. For this reason, the expression of the typical genes related to cell-cell and cell-matrix interactions, involved in several processes of differentiation, proliferation and migration, was analysed. In particular, we investigated the expression of two proteins; the E-cadherin CDH1 and the ITGB1BP1, a novel 200-aa protein that binds to the β1 integrin cytoplasmic domain. Cadherins are single-chain, calcium-dependent, transmembrane glycoproteins modulating cell-cell adhesion. CDH1 is characterised by an extracellular domain that allows interactions between

neighbouring cells.[33] Conversely, integrins are transmembrane receptors involved in cell-ECM matrix interactions. Among the several subunits of these receptors, the β1 integrin cytoplasmic domain is particularly investigated because it is connected to the binding of MSCs to bone and cartilage ECM proteins.[34,35] This domain is crucial for cell adhesion and binds to ITGB1BP1, that has also a function in bone differentiation and osteoblast mineralization.[36-38] In our study, the real-time PCR analysis showed an increase of ITGB1BP1 expression of about 2-fold in scaffold-free SASC-derived osteoblasts compared to undifferentiated SASCs. ITGB1BP1 expression increases of about 2-fold in osteoblasts from dXG-1-O-SASCs and dXG1.5-O-SASCs and decreases by about half in dXG 2.5-O, when compared to scaffold-free SASC-derived osteoblasts (control). Contrariwise, the CDH1 expression was downregulated in SASC-derived osteoblasts in comparison to undifferentiated SASCs, probably due to the loss of the spheroidal structure, and it was 12-fold up-regulated in dXG1-O-SASCs-derived cells, 7-fold up-regulated in the dXG1.5-O-SASCs-derived ones and unchanged in dXG-2.5-O-SASCs-derived cells with respect to their control. These results can be explained on the account of the interactions between hydrogels and cells. Both SEM and rheological analyses demonstrated a direct correlation between the increase in dXG concentration and the increase in network density, hence pore wall thickness, and an inverse correlation with average pore size and interconnectivity. During the incubation process with ODM, the hydrogel produced at low polymer concentration (dXG1-O) undergoes a maturation phase first, with an increase of polymer network density and stiffness during the first week, followed by a remodeling phase that opens up the pores and loosens the network mesh after the following two weeks. The maturation phase occurs also in the hydrogels produced at higher polymer concentration but displays significant effects in the mechanical properties only after 21 days of incubation, without leading to drastic changes in the scaffold morphology. MTS analysis evidences an inverse relationship between dXG concentration and final cell growth at T21; the hydrogel with the lowest polymer concentration being also the one where the cells likely find the required space to grow, divide and differentiate. CDH1 expression, that is related to cell-cell interaction, is inversely related to the increase of polymer concentration in the hydrogel. The highest value of CDH1 (12-fold increase) was observed for the cells from the dXG1-O scaffold, that has also the largest pores and highest cell viability. Conversely, ITGB1BP1 mRNA levels, that are related to cell-ECM interactions, are affected not only

by the cell proliferation ability but also by scaffolding ability of the hydrogel matrix. The presence of polymeric surfaces acting as artificial ECM is a pre-condition for cell-matrix adhesion, but if the surfaces are not part of an interconnected porous architecture, they may become an obstacle to further cell proliferation and scaffold colonization. For this reason, we observe a maximum of ITGB1BP1 mRNA levels expression for the intermediate polymer concentration, as a result of the counteracting effects related to substrate availability and cell growth.

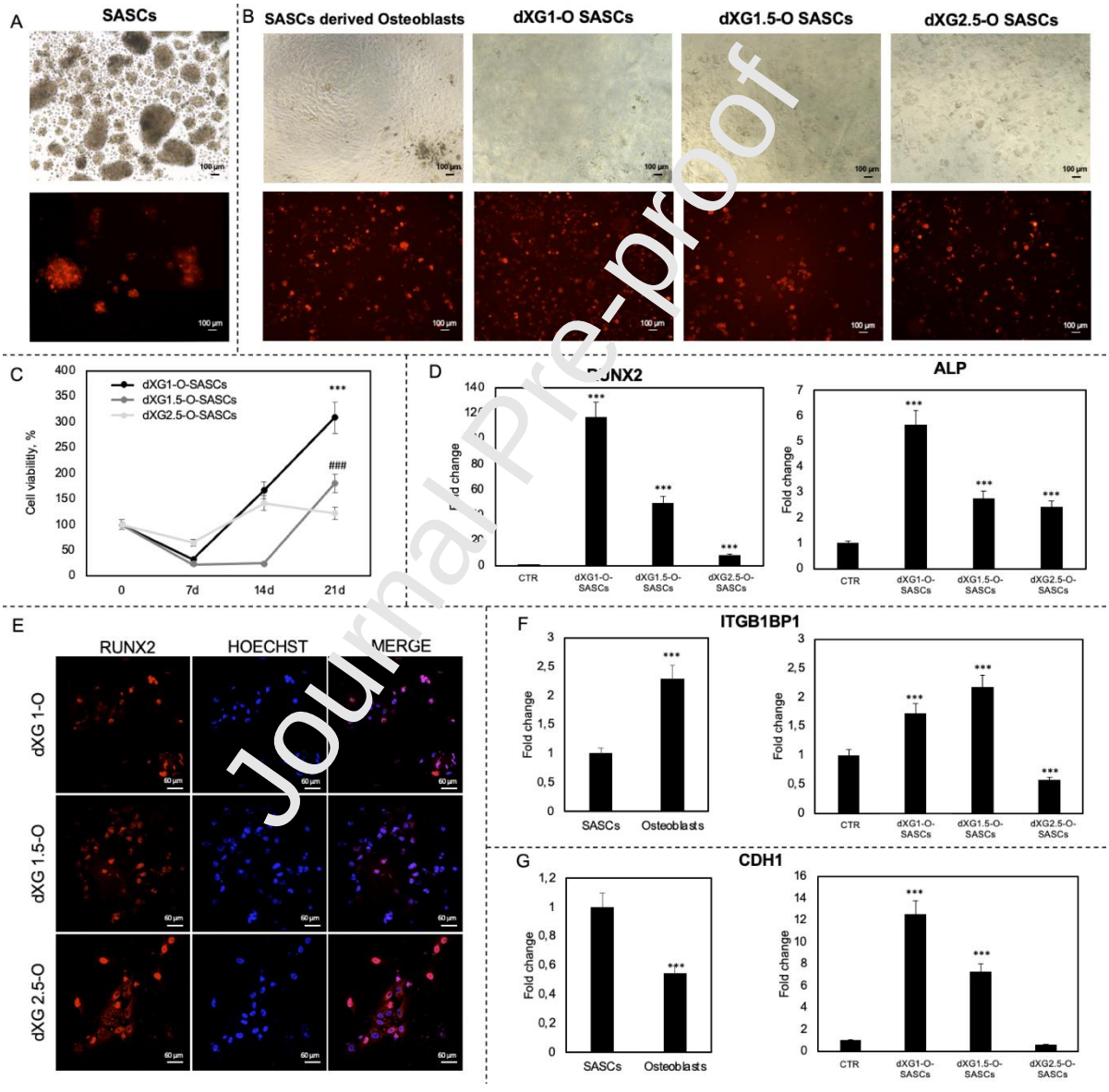

Figure 8. Representative optical and fluorescence (PKH26) microscope images of the A) SASCs at T0; B) SASC-derived osteoblasts incorporated in dXG1-O, dXG1.5-O and dXG2.5-O at T21; C) Cell viability at T7, T14 and T21 of *in vitro* culture; *** P<0.001 dXG1-O-SASCs vs dXG1.5-O-SASCs and dXG2.5-O-SASCs, ### P<0.001 dXG1.5-O-SASCs vs

dXG2.5-O-SASCs; D) Real Time PCR analysis of the RUNX2 and ALP genes; E) Immunofluorescence of RUNX2 (red), HOECHST (blue) and merge; F) Real time PCR analysis of the ITGB1BP1 and CDH1 in SASC-derived osteoblasts in dXG1-O, dXG1.5-O and dXG2.5-O.

3.4 Biological evaluation of chondroblastic differentiation

The same spheroids of **Figure 8A** were mixed with each of the three dXG dispersions and CDM and incubated for various times. The cell distribution in the scaffold after 21 days of *in vitro* chondroblastic culture is uniform also for these systems, as shown in the optical and fluorescence microscopy images presented in **Figure 9A**. Differently from before, MTS analysis of SASC-derived cells in dXG-C hydrogels did not show any reduction of cell viability at any time. In particular at T7, cell viability was unvaried in all scaffolds, at T14 increased for all, while at T21 presented a differentiated situation, with a 10-fold increase for dXG1-C, 3-fold for dXG1.5-C and 4-fold for dXG2.5-C (**Figure 9B**). Interestingly, the number of cells derived from SASCs, cultured within the hydrogels and conditioned with CDM, were significantly more than the SASC-derived osteoblasts cultured in analogous conditions. One possible explanation is provided by the SEM analysis of the scaffolds that shows evident differences among the morphologies of hydrogels incubated in the different cell culture media. In particular, with CDM dXG hydrogels present a more open and interconnected porosity that may leave the cells with more space to proliferate and better conditions for nutrients and catabolites exchange. Also, the relatively inferior performance of dXG1.5-C with respect to dXG2.5-C can be explained on the account of their different morphologies, more occluded for the first one than for the latter.

In analogy with the study carried out for the osteoblastic differentiation, we evaluated the chondroblastic differentiation of SASCs in the three hydrogels through specific gene and protein expression analyses at T21 of *in vitro* culture (see **Figure 9C, D**). Two typical chondroblastic markers have been analysed: SOX9 and COL10A1. The first is a key transcription factor in cartilage development, promotes cell survival and activates cartilage-specific genes, as reported in numerous studies.[39, 40] The second one is a marker of hypertrophic chondrocytes, which plays an important role in differentiation and matrix organization.[41,42,43] These genes were already found in a previous SASC characterization study. [19,31] For SASCs incorporated in dXG hydrogels, the real-time PCR analysis revealed a massive increase of SOX9 expression, about 5-fold

for all three scaffolds over the value of SASC-derived chondroblasts control group, confirming the occurrence of chondroblastic differentiation. Contrarywise, the levels of COL10A1 mRNA were the same of the control system in dXG1-C-SASCs and dXG1.5-C-SASCs and 5-fold down-regulated in dXG2.5-C-SASCs (see **Figure 9C**). These results suggest that SASC-derived chondrocytes have undergone complete maturation in dXG1-C and dXG1.5-C hydrogels as well as in the control system, while in the dXG2.5-C have probably not reached this condition, as suggested by the lower expression levels of COL10A1. To gather conclusive evidence on target cell-specific differentiation, we looked for the expression of SOX9 also through to immunofluorescence analysis. The z-stack visualization images at the confocal microscope confirmed the presence of only SOX9-positive cells, in all hydrogels (see **Figure 9D** for representative images).

The same real-time PCR analysis of genes related to cell-cell and cell-matrix interactions carried out for SASCs in dXG-C systems was conducted for SASCs in dXG-C systems at T21. As for ITGB1BP1 expression, SASC-derived chondroblasts showed a similar behaviour as the one observed for SASC-derived osteoblasts (see **Figure 9E**). Indeed, this gene is reported to be important as adhesive marker for cell-matrix interactions as well as for chondrocyte proliferation and differentiation, being associated to reduced apoptosis and involved in remodelling during cartilage repair.[44] The highest value of fold change obtained for dXG-1.5-C may have the same explanation as for dXG-1.5-O. Also in this case we have the highest proliferation for the hydrogel that is characterised by the lowest polymer concentration. Conversely, the CDH1 expression was downregulated in all SASC-derived chondroblasts including the control system (scaffold-free), in comparison to the undifferentiated SASCs (data not shown). These results make the CDH1 analysis unconclusive. In the development of the work, other cell-cell interaction markers for SASC-derived chondroblasts are going to be sought.

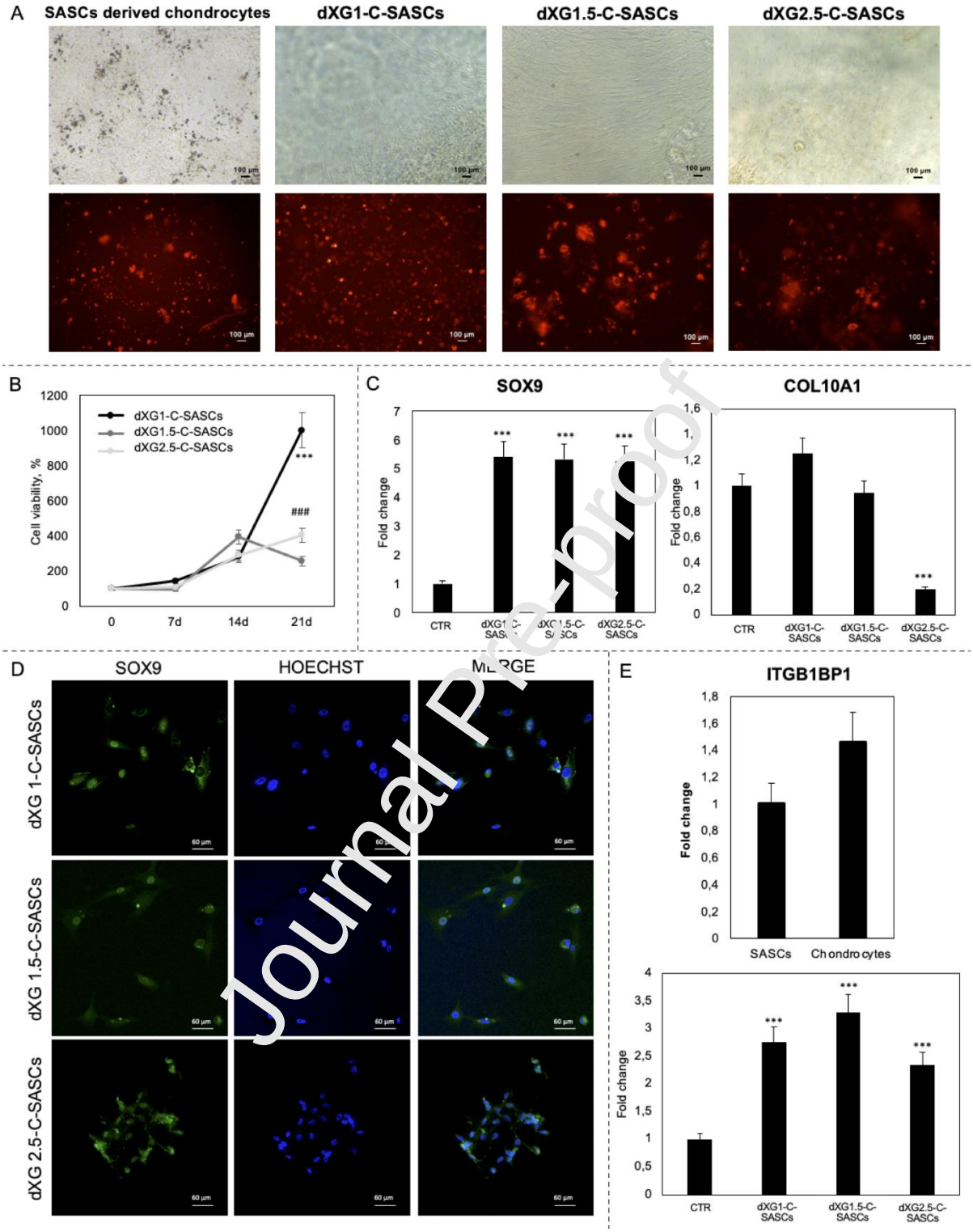

Figure 9. Representative optical and fluorescence (PKH26) microscope images of the A) SASC-derived chondroblasts incorporated in dXG1, dXG1.5 and dXG2.5 hydrogels, at T21 of *in vitro* culture. B) Cell viability of SASCs in dXG1-C, dXG1.5-C and dXG2.5-C hydrogels at T7, T14 and T21 of *in vitro* culture; *** P<0.001 dXG1-C-SASCs vs dXG1.5-C-SASCs and dXG2.5-C-SASCs, ### P<0.001 dXG1.5-C-SASCs vs dXG2.5-C-SASCs; C) Real Time PCR analysis of the SOX9 and COL10 genes; D) Immunofluorescence of SOX9

(green), HOECHST (blue) and merge; E) Real time PCR analysis of ITGB1BP1in SASC-derived chondroblasts incorporated in dXG1-C, dXG1.5-C and dXG2.5-C hydrogels.

3.5 Injectability of dXG dispersions mixed with SASCs

Shear viscosity measurements as function of shear rate have been performed in order to characterize the flow properties of the dXG dispersions mixed with SASCs. The measurements were carried out on systems freshly mixed with each of the two conditioning media and compared to the analogous systems without cells. The flow curves, reported in **Figure 10A-B**, show the typical features of pseudo-plastic fluids. The viscosity decreases with the increase of the shear rate, as a result of the decrease in number of entanglements when chains align parallel to the flow direction. The increase in polymer concentration leads to an overall higher apparent viscosity and a more marked non-Newtonian behavior. The presence of SASCs in the formulation and the nature of the culture medium do not significantly affect the apparent viscosity, especially at higher shear stresses.

The injectability of liquid formulations can be affected by the needle geometry, i.e. inner diameter, length, shape of the opening, as well as by the inner surface (composition and finish) of the syringe. As far as pre-filled syringes are concerned, common needle configurations, e.g. for articular injection of viscous formulations, are G21 and G23.[45] The evaluation of the injectability can be addressed by establishing the force to initiate and maintain the plunger movement down the barrel. Force-displacement plots, obtained applying a constant displacement rate to the plunger of the syringe and measuring the resulting force (F) as function of the displacement, are provided as supplementary material (see **Figure S2**). In **Table 1**, the following parameters derived from the plots are presented: (i) the plunger-stopper break loose force (PBF), that is the force required to initiate the movement of the plunger; (ii) the maximum force (F_{max}), that is the highest force measured before the plunger finishes its course at the front end of the syringe; and (iii) the dynamic glide force (DGF_{av}), that is the average force required to sustain the movement of the plunger to expel the content of the syringe. When the syringe barrel was filled with water, both in the presence and in the absence of the needle, the measured force was always 1N, therefore the friction of the syringe plunger is negligible. dXG1-C presents higher PBF, F_{max} and DGF_{av} values than the corresponding ones for dXG1-O. dXG1.5-C and dXG1.5-O as well as dXG2.5-C

and dXG2.5-O present comparable values with the respective PBF, F_{max} and DGF_{av} parameters. The force increases with the polymer concentration, but it is always well below the maximum acceptable injection force by the average medical operator (F_{max} = 40 N) and fulfils the requirement of most types of injection devices, that is F_{max} < 20 N. [46] In consideration of the obtained flow curves, F_{max} is not expected to increase in the presence of SASCs.

In order to assess the effect of the injection on the hydrogel structure, the mixtures with or without cells were injected directly on the rheometer plate through a G23 syringe needle and subjected to frequency sweep measurements. The same systems spooned on the plate were also tested for comparison. The G' and G" curves are shown in **Figure 10C-H**. The mechanical spectra do not evidence any significant effect of the injection in systems without cells formulated with each of the two media. The presence of SASCs exerts always a slight reinforcing effect on the non-injected hydrogels, while the injected systems containing SASCs do not show a clear trend but the differences with respect to the non-injected systems are never substantial. Cell viability after injection of SASCs mixed with dXG, ODM or CDM a T1 did not change in comparison to the non-injected counterparts (**Table 1**), as also observed for SASCs mixed with dXG and stem cell medium (SCM).[20] These data together with the rheological analysis demonstrate the injectability of this novel combination of cells and biomaterials opening up the prospect for clinical applications in bone and cartilage repair.

Table 1. PBF, F_{max} and DGF_{av} values and cell viability percentages for dXG1, dXG1.5 and dXG2.5 mixed with CDM and ODM.

Systems	PBF [N]	Fmax [N]	DGFav [N]	Cell viability [%]
dXG1-C	6.0	6.9	5.7	103
dXG1-O	2.5	3.7	3.4	101
dXG1.5-C	8.0	10	9.1	111
dXG1.5-O	10	14	11	109
dXG2.5-C	17	20	19	102
dXG2.5-O	15	19	17	103

4. Conclusion

Xyloglucan is a relatively inexpensive and biocompatible polymer that, when partially degalactosylated and dispersed into aqueous media at relatively low concentration, quickly sets at body temperature into soft, conformable and durable hydrogels. Its dispersions are easy to inject at room temperature, also when mixed with SASCs. The transient exposure to shear stresses during the syringe injection, despite of the very small gauge needle used, showed no effects on cell viability and did not significantly change the hydrogel structure. Mixing the polymer with culture media containing various growth factors and hormones which stimulate cell differentiation did not detrimentally affect dXG body temperature-induced gelation. Indeed, injectability and fast gelation with no recourse to crosslinking agents or initiators are key features for in-situ forming scaffolds. The hydrogels also retain the chemical and biological molecules they have been formulated with making them available to the incorporated cells and active, becoming highly specific, function-tailored artificial niches. When dXG is formulated with an osteoblastic differentiation-inductive medium, it grants complete differentiation of the incorporated stem cell spheroids into the target cell lineage. Differentiation leads to significant proliferation and uniform scaffold colonization, especially for dXG1-O, when the polymer is at its lowest concentration and pores are larger and more interconnected. Interestingly, a 100-fold increase of expression of RUNX2 was measured. Being RUNX2 an important transcription factor of many genes related to osteoblastic differentiation; further work is needed to investigate in more detail its pathway. When dXG is formulated with a chondrocyte differentiation-inductive medium, the differentiation is exclusively into chondrocytes and is associated to a remarkable 10-fold increase of cell viability at T21, for dXG1-C. All hydrogels undergo a process of network remodelling when incubated at 37°C, and either a complete or only partial erosion at a slow rate when exposed to a large volume of aqueous solutions. Their soft and dynamic structure offer adequate support to cells, allows their spreading and grant favourable conditions for their viability. All the results so far gathered strongly encourage to progress with the biological evaluation of these systems on animal models and, at the same time, to explore more in detail eventual specific interactions between SASCs and SASC-derived cells with dXG.

If the in vivo evaluations will confirm the regenerative effects coming from the administration of autologous SASCs with dXG, this approach could become a clinically translatable treatment option for cartilage or bone defect with suitable characteristics, to activate or accelerate tissue regeneration processes, making the return to functional work and sport possible in shorter time and limiting the risk of permanent moderation of activities.

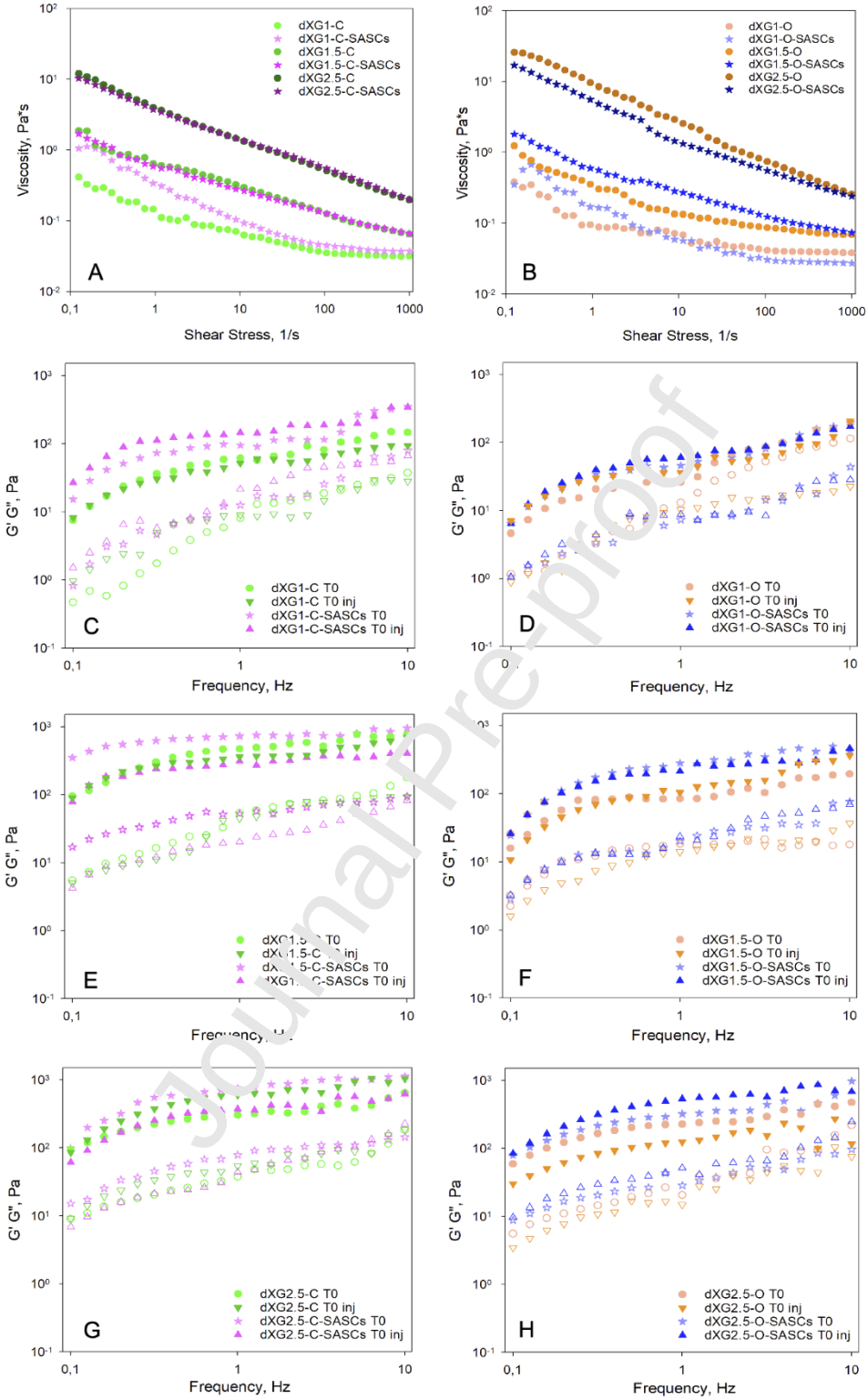

Figure 10. Shear viscosity of dXG1, dXG1.5 and dXG2.5 mixed with CDM (A) and with ODM (B) with and without SASCs as a function of the shear rate; storage modulus, G' (full dot), and loss modulus, G" (hollow dot), of dXG1 (C-D), dXG1.5 (E-F) and dXG2.5 (G-H) hydrogels conditioned with ODM and CDM, either not-injected or injected (inj) as a function of the frequency.

References

[1] G. Chamberlain, J. Fox, B. Ashton, J. Middleton, Concise Review: Mesenchymal Stem Cells: Their Phenotype, Differentiation Capacity, Immunological Features, and Potential for Homing. *Stem Cells* **2007**, 25, 2739-2749. DOI: 10.1634/stemcells.2007-0197

[2] S. G. Almalki, D. K. Agrawal, Key transcription factors in the differentiation of mesenchymal stem cells. *Differentiation* **2016**, 92, 41-51. DOI: 10.1016/j.diff.2016.02.005 and references herein.

[3] J.M. Gimble, F. Guilak, Differentiation potential of adipose derived adult stem (ADAS) cells. *Curr Top Dev Biol* **2003**, 58, 137-160. DOI: 10.1016/s0070-2153(03)58005-x.

[4] J.K. Fraser, I. Wulur, Z. Alfonso, M.H. Hedrick, Fat tissue: an underappreciated source of stem cells for biotechnology *Trends Biotechnol* **2006**, 24, 150-154. DOI: 10.1016/j.tibtech.2006.01.010.

[5] L. Aust, B. Devlin, S.J. Foster, Y.D. Halvorsen K Hicok, T. du Laney, A Sen, G D Willingmyre, J M Gimble, Yield of human adipose-derived adult stem cells from liposuction aspirates. *Cytotherapy* **2004**, 6, 7-14. DOI: 10.1080/14653240310004539.

[6] B. Parekkadan, J. M. Milwid, Mesenchymal Stem Cells as Therapeutics *Annu. Rev. Biomed. Eng.* **2010**, 12, 87-117. DOI: 10.1146/annurev-bioeng-070909-105309.

[7] M. Satuè, C. Schuler, N. Gimeno, R. G. Erben, Intra-articularly injected mesenchymal stem cells promote cartilage regeneration, but do not permanently engraft in distant organs. *Sci. Rep.* **2019**, 9, 10153. DOI: 10.1038/s41598-019-46554-5.

[8] J. S. Hyun, M. C. Tran, V. W. Wong, M. T. Chung, D. D. Lo, D. T. Montoro, D. C. Wan, M. T. Longaker, Enhancing stem cell survival in vivo for tissue repair. *Biotechnol. Adv.* **2013**, 31, 736-743. DOI: 10.1016/j.biotechadv.2012.11.003.

[9] E. Fuchs, T. Tumbar, G. Guasch, Socializing with the Neighbors: Stem Cells and Their Niche, *Cell* **2004**,16 (6), 769-778. DOI: 10.1016/S0092-8674(04)00255-7.

[10] H. Donnelly, M. Salmeron-Sanchez, M. J. Dalby, Designing stem cell niches for differentiation and self-renewal. *J. R. Soc. Interface* **2018**, 15(145), 20180388. DOI: 10.1098/rsif.2018.0388.

[11] S. C. De Groot, K. Sliedregt, P. P. G. Van Benthem, M. N. Rivolta, M. A. Huisman, Building an Artificial Stem Cell Niche: Prerequisites for Future 3D-Formation of Inner Ear Structures-Toward 3D Inner Ear Biotechnology. *Anatomical Record* **2020** (Hoboken, N.J. : 2007), 303(3), 408-426. DOI: 10.1002/ar.24067.

[12] A. J. Engler, S. Sen, H. L. Sweeney, D. E. Discher, Matrix elasticity directs stem cell lineage specification. *Cell* **2006**, 126, 677-689. DOI: 10.1016/j.cell.2006.06.044.

[13] M. Nii, J. H. Lai, M. Keeney, L. H. Han, A. Behn, G. Imanbayev, F. Yang. The effects of interactive mechanical and biochemical niche signaling on osteogenic differentiation of adipose-derived stem cells using combinatorial hydrogels. *Acta Biomater.* **2013**, 9, 5475-5483. DOI: 10.1016/j.actbio.2012.11.002.

[14] E. V. Alakpa, V. Jayawarna ,A. Lampel, K. V. Burgess ,C. C.West,S. C. J. Bakker S. Roy, N. Javid, S. Fleming D. A. Lamprou,J. Yang, A. Miller,A. J. Urquhart, P. W. J. M. Frederix,Neil T.Hunt, B. Péault, R. V.Ulijn, M. J.Dalby, *Chem* **2016**, 1, 298-319. DOI: 10.1016/j.chempr.2016.07.001.

[15] B. Lindroos, R. Suuronen, S. Miettinen The Potential of Adipose Stem Cells in Regenerative Medicine *Stem Cell Rev. Rep.* **2011**, 7(2), 269-291. DOI:10.1007/s12015-010-9193-7.

[16] A. B. Di Stefano, F. Grisafi, M. Perez-Alea, M. Castiglia, M. Di Simone, S. Meraviglia, A. Cordova, F. Moschella, F. Toia, Cell quality evaluation with gene expression analysis of spheroids (3D) and adherent (2D) adipose stem cells. *Gene* **2021**, 768, 145269. DOI: 10.1016/j.gene.2020.145269.

[17] A. B. Di Stefano, L. Montesano, B. Belmonte, A. Gulino, C. Gagliardo, A. M. Florena, G. Bilello, F. Moschella, A. Cordova, A. A. Leto Barone, F. Toia, Human Spheroids from Adipose-Derived Stem Cells Induce Calvarial Bone Production in a Xenogeneic Rabbit Model. *Ann. Plast. Surg.* **2021**, 86(6), 714-720. DOI: 10.1097/SAP.0000000000002579.

[18] S. S. Ho, K. C. Murphy, B. Y. K. Binder, C. B. Vissers, J. K. Leach, Increased Survival and Function of Mesenchymal Stem Cell Spheroids Entrapped in Instructive Alginate Hydrogels *Stem Cells Transl. Med.* **2016**, 5,773-781. DOI: 10.5966/sctm.2015-0211.

[19] A. B. Di Stefano, A. A. Leto Barone, A. Giammona, T. Apuzzo, P. Moschella, S. Di Franco, G. Giunta, M. Carmisciano, C. Eleuteri, M. Todaro, F. Dieli, A. Cordova, G. Stassi, F. Moschella, Identification and Expansion of Adipose Stem Cells with Enhanced Bone Regeneration Properties. *J. Regen. Med.* **2016**, 5, 1. DOI: 10.4172/2325-9620.1000124.

[20] F. Toia, A. B. Di Stefano, E. Muscolino , M. A. Sabatino, D. Giacomazza, F. Moschella, A. Cordova, C. Dispenza, In-situ gelling xyloglucan formulations as 3D

artificial niche for adipose stem cell spheroids, *Int. J. Biol. Macromol.* **2020**, 165, 2886-2899. DOI: 10.1016/j.ijbiomac.2020.10.158.

[21] A. Mishra, A. V. Malhotra, Tamarind xyloglucan: a polysaccharide with versatile application potential *J. Mater. Chem.* **2009**, 19, 8528-8536. DOI: 10.1039/B911150F.

[22] S. Najmudin,C. I. P. D. Guerreiro, A. L.Carvalho, J. A. M. Prates, M A.S.Correia, V. D. Alves, L. M.A.Ferreira,M. J. Romão,H. J.Gilbert, D. N.Bolam, C. M. G. A. Fontes, Xyloglucan Is Recognized by Carbohydrate-binding Modules That Interact with β-Glucan Chains. *J. Biol. Chem.* **2006**, 281(13), 8815-8828. DOI: 10.1074/jbc.M510559200.

[23] D. M. Zacharski, S. Brandt, S. Esch, S. König, M. Mormann, G. Ulrich-Merzenich, A. Hensel, Xyloglucan from Tropaeolum majus Seeds Induces Cellular Differentiation of Human Keratinocytes by Inhibition of EGFR Phosphorylation and Decreased Activity of Transcription Factor CREB, *Biomacromolecules* **2015**, 16, 2157-2167. DOI: 10.1021/acs.biomac.5b00553.

[24] A. K. A. S. Brun-Graeppi, C Richard, M. Bessodes, D. Scherman, T. Narita, G. Ducouret, O. Merten, Study on the sol–gel transition of xyloglucan hydrogels. *Carbohydr. Polym.* **2010,** 80(2), 555-562. DOI: 10.1016/j.carbpol.2009.12.026.

[25] S. Todaro, C. Dispenza, M.A. Sabatino, M.G. Ortore, R. Passantino, P.L. San Biagio and D. Bulone Temperature-induced self-assembly of degalactosylated xyloglucan at low concentration. *J. Polym. Sci. Part B: Polym. Phys.* **2015**, 53, 1727-1735. DOI:10.1002/polb.23895

[26] M. Shirakawa, K.Yamatoya, K. Nishinari, Tailoring of xyloglucan properties using an enzyme, *Food Hydrocolloids* **1998**, 12(1), 25-28. DOI: 10.1016/S0268-005X(98)00052-6.

[27] K.J. Livak, T.D. Schmittgen, Analysis of relative gene expression data using real-time quantitative PCR and the 2(-Delta Delta C(T)) *Method. Methods*. **2001**, 25(4), 402-408. DOI: 10.1006/meth.2001.

[28] M. Han, Y. Liu, F. Zhang, D. Sun, J. Jiang, Effect of galactose side-chain on the self-assembly of xyloglucan macromolecule, *Carbohydr. Polym.* **2020**, 246, 116577, DOI:10.1016/j.carbpol.2020.116577.

[29] T. Komori, Regulation of Proliferation, Differentiation and Functions of Osteoblasts by Runx2. *Int. J. Mol. Sci.* **2019**, 20(7), 1694. DOI: 10.3390/ijms20071694.

[30] E. Birmingham, G. L. Niebur, P. E. McHugh, G. Shaw, F. P. Barry, L. M. McNamara, Osteogenic differentiation of mesenchymal stem cells is regulated by osteocyte and

osteoblast cells in a simplified bone niche. *Eur Cell Mater* **2012**, 23, 13-27. DOI: 10.22203/ecm.v023a02.

[31] A. B. Di Stefano, F. Grisafi, M. Castiglia, A. Perez, L. Montesano, A. Gulino, F. Toia, D. Fanale, A. Russo, F. Moschella, A. A. Leto Barone, A. Cordova, Spheroids from adipose-derived stem cells exhibit an miRNA profile of highly undifferentiated cells *J. Cell Physiol*. **2018**, 233(11), 8778-8789. DOI: 10.1002/jcp.26785.

[32] E. Wrobel, J. Leszczynska, E. Brzoska, The Characteristics Of Human Bone-Derived Cells (HBDCS) during osteogenesis in vitro. *Cell. Mol. Biol. Lett.* **2016**, 21, 26-41. DOI: 10.1186/s11658-016-0027-8.

[33] L. Li, S. A. Bennett, L. Wang, Role of E-cadherin and other cell adhesion molecules in survival and differentiation of human pluripotent stem cells. *Cell. Adh. Migr.* **2012**, 6(1), 59-70.

[34] D. Zwolanek, M. Flicker, E. Kirstätter, F. Zaucke, C. J. van Osch, R. G. Erben, β1 Integrins Mediate Attachment of Mesenchymal Stem Cells to Cartilage Lesions. *Biores. Open Access* **2015**, 4(1), 39 39-53. DOI: 10.1089/biores.2014.0055.

[35] K. Song, T. J. Park, Integrin signaling in cartilage development *Anim. Cells Syst.* **2014**, 18(6), 365-371. DOI: 10.1080/19768354.2014.987319.

[36] D. D. Chang, C. Wong, H. Smith, J. Liu, ICAP-1, a novel beta1 integrin cytoplasmic domain-associated protein, binds to a conserved and functionally important NPXY sequence motif of beta1 integrin. *J. Cell. Biol*. **1997**, 138(5), 1149-1157. DOI: 10.1083/jcb.138.5.1149.

[37] M. Brunner, A. Millon-Frémillon, G. Chevalier, I. A. Nakchbandi, D. Mosher, M. R. Block, C. Albigès-Rizo, D. Bouvard, Osteoblast mineralization requires β1 integrin/ICAP-1–dependent fibronectin deposition. *J.Cell. Biol*, **2011**, 194(2), 307-322. DOI: 10.1083/jcb.201007108.

[38] I. D. Campbell, M. J. Humphries, Integrin structure, activation, and interactions. *Cold Spring Harbor Perspect. Biol*. **2011**, 3(3), a004994. DOI: 10.1101/cshperspect.a004994.

[39] Z. Yang, C. Y. Huang, K. A. Candiotti, X. Zeng, T. Yuan, J. Li, H. Yu, S. Abdi, Sox-9 facilitates differentiation of adipose tissue-derived stem cells into a chondrocyte-like phenotype in vitro *J. Orthop. Res.* **2011**, 29, 1291-1297. DOI: 10.1002/jor.21336.

[40] V. Lefebvre, M. Dvir-Ginzberg, SOX9 and the many facets of its regulation in the chondrocyte lineage. *Connect. Tissue Res.* **2017**, 58, 2-14. DOI: 10.1080/03008207.2016.1183667.

[41] J. Gu, Y. Lu, F. Li, L. Qiao, Q. Wang, N. Li, J. A. Borgia, Y. Deng, G. Lei, Q. Zheng, Identification and characterization of the novel Col10a1 regulatory mechanism during chondrocyte hypertrophic differentiation. *Cell Death Dis* **2014**, 5(10), e1469. DOI: 10.1038/cddis.2014.444.

[42] C. A. Knuth, E. Andres Sastre, N. B. Fahy, J. Witte-Bouma, Y. Ridwan, E. M. Strabbing, M. J. Koudstaal, J. van de Peppel, E. B. Wolvius, R. Narcisi, E. Farrell, Collagen type X is essential for successful mesenchymal stem cell-mediated cartilage formation and subsequent endochondral ossification, *Eur. Cell. Mater*. **2019**, 38, 106-122. DOI: 10.22203/eCM.v038a09, hdl.handle.net/1765/119811.

[43] J. Xu, W. Wang, M. Ludeman, K. Cheng, T. Hayami, J. C. Lotz, S. Kapila, Chondrogenic Differentiation of Human Mesenchymal Stem Cells in Three-Dimensional Alginate Gels. *Tissue Engineering: Part A.* **2008,** 14, 667-80. doi: 10.1089/tea.2007.0272

[44] S. Zhang, P. Liu, L. Chen, Y. Wang, Z. Wang, B. Zhang, The effects of spheroid formation of adipose-derived stem cells in a microgravity bioreactor on stemness properties and therapeutic potential. *Biomaterials* **2015**, 41, 15-25. DOI: 10.1016/j.biomaterials.2014.11.013

[45] M. B. Stephens, A. Beutler, F. C. O'Connor, Musculoskeletal injections: a review of the evidence. *Am. Fam.Physician* **2008**, 78, 971-976. PMID: 18953975.

[46] R.P. Watt, H. Khatri, A.R.C. Dibble, Injectability as a function of viscosity and dosing materials for subcutaneous administration. *Int J Pharm.* **2019**, 554, 376-386. doi: 10.1016/j.ijpharm.2018.11.012

Conflict of interest

The authors declare no conflict of interest.

Acknowledgements

C.D. acknowledges the FFR 2019/2020 grant of the University of Palermo.

F.T. acknowledges the GR-2016-02364931 grant.

Author Contributions

E.M. and A.B.D.S. contributed equally to this work. E.M. synthesized the material, performed the material characterization, analyzed the data and drafted the manuscript. A.B.D.S designed the biological characterization, analyzed the data and drafted the manuscript. M.T. performed the cellular experiments and drafted the manuscript. M.A.S and

D.G. directed the study and revised the manuscript. F.M., A.C. and F.T. acquired funding and directed the study. C.D. acquired funding, designed and directed the study and revised the manuscript.

Declaration of interests

☒ The authors declare that they have no known competing financial interests or personal relationships that could have appeared to influence the work reported in this paper.

☐The authors declare the following financial interests/personal relationships which may be considered as potential competing interests:

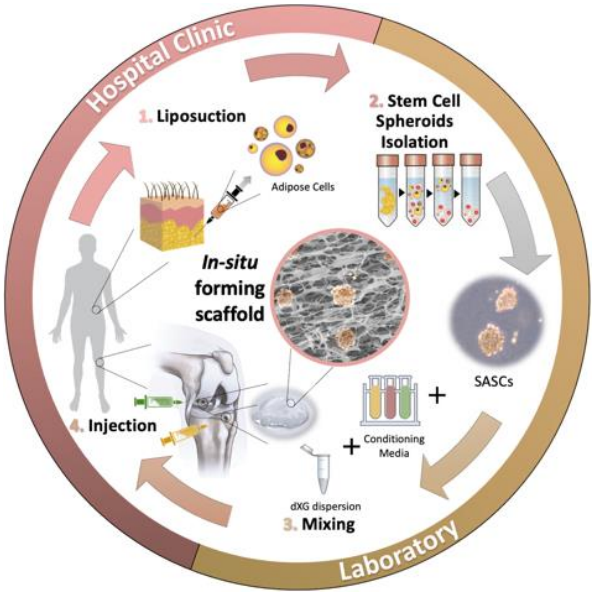

Graphical abstract

Highlights

- Partially degalactosilated xyloglucan (dXG) dispersed in inductive media rapidly set into gels at 37°C
- Increasing dXG concentration reduces the time to gel and increases the gel strength
- The physical networks undergo significant reorganization during incubation for 21 days
- Gels provide control of stem cell differentiation towards a single cell lineage
- 1%w dXG gels show 300% viability for osteocytes and 1000% in chondrocytes after 21 days.
- Cells mixed with the gels and injected through small gauge syringe needles retain viability